Tantalum diffusion barrier grown by inorganic plasma-promoted chemical vapor deposition: Performance in copper metallization

Alain E. Kaloyeros, [a] Xiomeng Chen, Sarah Lane, and Harry L. Frisch
New York State Center for Advanced This Film, Technology and Department of Physics, The University at Albany-SUNY, Albany, New York 12222

Barry Arkles
Gelest Inc., Tullytown, Pennsylvania 19007

(Received 1 February 1999; accepted 13 September 2000)

As-deposited and annealed tantalum films, grown by plasma-promoted chemical vapor deposition (PPCVD) using pentabromotantalum and hydrogen as coreactants, were evaluated as diffusion barriers in copper metallization. Stacks consisting of 500-nm-thick sputtered Cu/55-nm-thick untreated PPCVD Ta/Si were annealed in argon in the range 450 to 650 °C, in 50 °C intervals, along with sputtered Cu/preannealed PPCVD Ta/Si and sputtered Cu/sputtered Ta/Si stacks of identical thickness. Pre- and postannealed stacks were characterized by x-ray photoelectron spectroscopy, Auger electron spectroscopy, Rutherford backscattering spectrometry, hydrogen profiling, x-ray diffraction, atomic force microscopy, sheet resistance measurements, and Secco chemical treatment and etch-pit observation by scanning electron microscopy. The sputtered and preannealed PPCVD Ta films acted as viable diffusion barriers up to 550 °C while the as-deposited PPCVD Ta films failed above 500 °C. In all cases, breakdown occurred through the migration of Cu into Si, rather than an interfacial reaction between Ta and Si, in agreement with previously reported results for sputtered Ta films. The accelerated barrier failure for as-deposited PPCVD Ta might have been caused by the presence of approximately 20 at. % hydrogen in the as-deposited PPCVD Ta, an observation which was supported by the enhanced performance of the same PPCVD Ta films after annealing-induced hydrogen removal.

1. INTRODUCTION

The successful incorporation of copper-based metallization schemes in emerging ultra-large-scale-integration (ULSI) computer chip device generations requires the identification and development of viable diffusion barrier/adhesion promoter material technologies.[1] These “liner” materials are required to prevent undesirable diffusion and interaction between copper and the semiconductor and dielectric regions of the chip. In particular, it is well known that the presence of copper in silicon leads to the formation of deep trap levels that cause serious device degradation and failure. As device size continues its trend toward smaller features, the liners must provide enhanced barrier performance at reduced thickness in order to maximize space availability for the actual conductor.

[a] Address all correspondence to this author.

Various refractory material systems primarily transition metals and their binary and ternary nitrides, have been extensively investigated for liner applications in copper metallization.[2] In this respect, tantalum-based material systems are perhaps the most studied because of their highly desirable physical, chemical, mechanical, and electrical properties These advantageous properties are further enhanced by the thermodynamic stability of Ta and its nitrides with respect to Cu, given the absence of Cu-Ta or Cu-N compounds.

Experimental studies have demonstrated viable performance for Ta and its alloys against Cu diffusion. For instance, a 50-nm-thick sputtered Ta film has provided excellent resistance to Cu diffusion up to 550°C for 1 h.[4,5] However, conventional physical vapor deposition (PVD) methods, such as sputtering, are line of sight techniques. As such, they are inherently incapable of conformal step coverage in sub-quarter-micron device topographies, even though higher step

 © 2000 Materials Research Society

coverage was observed for Ta in comparison with Ti. The improved coverage was attributed to increased sputtering directionality due to the higher mass of the Ta ion.[6] Modified PVD techniques, such as ionized sputtering, provide a viable solution to the conformality problem. However, concerns over the long-term extendibility of ionized sputtering, and integration issues pertaining to the effects of ionized PVD processing on the mechanical and structural reliability of fluorinated low dielectric constant materials, have generated appreciable interest in alternate linear processing technologies.

In view of these considerations, work by the authors has focused on the identification and development of low-temperature chemical vapor deposition (CVD) techniques for Ta and its nitrides. In many CVD applications involving fine line geometries, good conformality can be achieved by exploiting the catalytic role that the substrate surface plays in the deposition process, leading to the identification of experimental conditions that are conducive to optimized reaction pathways. The overall approach is to ensure equal probability for precursor species adsorption and reaction across all of the complex topographical surfaces of device via and trench structures, thereby leading to conformal step coverage.

In this context, a low-temperature plasma-promoted CVD (PPCVD) process has been identified and optimized. The process combines the use of tantalum pentabromide ($TaBr_5$) with hydrogen plasma to produce Ta thin films at or below 450 °C.[7] As described in a previous report,[7] tantalum pentabromide was selected because of the low dissociation energy of Ta-Br bonds. This feature, when combined with the use of a plasma to generate active hydrogen species for the efficient reduction of the $TaBr_5$ molecule, leads to Ta formation at low temperatures. As a result, Ta films can be grown at 450 °C with Br contamination below 2.7 at.% and preannealing hydrogen inclusion of about 20 at.%.[7] In this report, the results of a study of the stability of H and Br in as-deposited and annealed PPCVD Ta films are presented, and the performance of these films as diffusion barriers in Cu metallization is discussed.

II. EXPERIMENTAL DETAILS

A. Description of processing conditions

The 550-Å-thick PPCVD and PVD Ta films were grown on Si(100) substrates. Prior to Ta deposition, the Si substrates received a standard organic cleaning process consisting of a l-min immersion in baths of trichloroethylene, acetone, and methanol. This was followed by a l-min exposure to a 10% aqueous HF solution to remove the native oxide. All samples were subsequently *in situ* plasma cleaned in their respective CVD and PVD processing modules prior to actual deposition. In the case of PPCVD Ta, processing was performed in a custom-designed, warm-wall plasma-capable, stainless steel CVD reactor. The deposition process has been described in detail elsewhere.[7] In the case of PVD Ta, conventional sputter deposition was carried out in a commercial Varian MB2 cluster tool system. Table I presents the relevant process parameters for the deposition of the PPCVD and PVD Ta films studied here.

Following the deposition step, the PVD and PPCVD Ta films were exposed to 30-min anneals each in argon at temperatures of 450, 500, 550, 600, and 650 °C. Annealing was performed in l-atm argon, with the argon gas flow being controlled by an MKS model 1159C (MKS Instruments, Andover, MA) electronic mass flow controller. Accurate determination of the annealing temperature was achieved by placing a thermocouple inside the annealing furnace in close proximity of the samples being annealed. The thermocouple was connected to an Omega type CN2002 (Omega Engineering, Stamford, CT) electronic temperature controller, which monitored the sample temperature in real time and provided control of the furnace temperature in a closed feedback loop. The goal of this part of the work was to investigate and document any thermally induced compositional or structural changes in the Ta films that might influence their behavior in the subsequent Cu diffusion barrier studies.

The 500-nm-thick Cu films were formed by conventional sputtering on as-deposited PVD, untreated PPCVD Ta, and preannealed PPCVD Ta to form Cu/Ta/Si contact systems. For the

TABLE I. Summary of process parameters for PPCVD Ta, PVD Ta, and PVD Cu films.

PPCVD Ta		PVD Ta		PVD Cu	
Reactant gas (flow rate)	H_2 (50 sccm)	Sputtering gas (flow rate)	Ar (50 sccm)	Sputtering gas (flow rate)	Ar (40 sccm)
Deposition pressure	0.7 torr	Deposition pressure	5 mtorr	Deposition pressure	4 mtorr
Base pressure	10^{-6} torr	Base pressure	10^{-8} torr	Base pressure	~10^{-8} torr
Substrate temp.	450 °C	Substrate temp.	25 °C	Substrate temp.	25 °C
Source temp.	160 °C	Plasma power (dc)	2 kW	Plasma power (dc)	2 kW

 © 2000 Materials Research Society

preannealed PPCVD Ta films thermal treatment was carried out in l-atm argon at 450 °C for 30 min prior to Cu deposition. Cu deposition was carried out in a commercial CVC cluster tool, using the process parameters listed in Table I. All PPCVD and PVD Ta samples were exposed to air prior to Cu deposition, leading to the formation of an ultrathin surface tantalum oxide layer. As a result, the samples were subjected to a brief argon-plasma treatment in the PVD chamber prior to the PVD Cu step. Subsequent Auger electron spectroscopy (AES) and x-ray photoelectron spectroscopy (XPS) depth profiles studies did not detect any oxide phase at the interfaces of the Cu/PVD Ta and Cu/PPCVD Ta films. This result implies that either the thickness of the remaining oxide layer was below the spatial resolution of XPS and AES or that the oxide layer was completely removed under the influence of sputtering with active argon ions in the PVD Cu chamber. All Cu/Ta stacks were subsequently annealed in Ar ambient for 30 min each at 450, 500, 550, 600, and 650 °C. Accurate real-time measurement of the annealing temperature was achieved through an electronically controlled, closed feedback loop as described earlier.

B. Description of characterization techniques

Characterization of film microchemical, microstructural, and diffusion barrier properties were carried out using the analytical facilities of the New York State Center for Advanced Thin Film Technology. For this purpose, the work employed AES, XPS, Rutherford backscattering spectrometry (RBS), x-ray diffraction (XRD), atomic force microscopy (AFM), four-point resistivity probe, nuclear reaction analysis (NRA) for hydrogen profiling, and scanning electron microscopy (SEM).

XPS and RBS were employed to determine film compositional characteristics. XPS measurements employed a Physical Electronics PHI 5500 (Flying Cloud, MN) Multi-technique System. A magnesium x-ray source was employed at voltage and power ratings of respectively 15 kV and 300 W. High-resolution XPS spectra were collected at a pass energy of 23.50 eV to allow the resolution of specific core level photoelectron peaks. RBS spectra were taken at a primary He^+ ion beam energy of 2 MeV. The resulting data were calibrated with bulk gold and carbon samples. In addition, nuclear reaction analysis for hydrogen profiling was carried out using the nuclear reaction $^{15}N(p, \alpha\gamma)^{12}C$ with resonance energy of 6.385 + 0.005 MeV.

Analysis of film texture and identification of phases was made using XRD on a Scintag XDS 2000 (Cupertino, CA) x-ray diffractometer. A copper $K\alpha$ x-ray source was employed for the generation of x-rays at a typical operating power of 1.8 kW. This value corresponded to a primary current and voltage of respectively 40 mA and 45 kV. XRD data was obtained using normal incidence and 5° grazing angle geometries.

Imaging studies were carried out using SEM and AFM. SEM was carried out on a Zeiss DSM 940 microscope at a 20-keV primary electron beam energy. AFM was performed on a Digital Instruments Nanoscope III multimode scanning probe microscope. Data were collected in tapping mode AFM with Si cantilevers at resonance frequencies in the range of 200 to 300 kHz. Root-mean-square (rms) surface roughness was calculated as the standard deviation of the mean height of surface topographies. Average surface grain size was determined using established AFM statistical averaging techniques for the height and slope of surface topographies, with defined grain boundaries being employed to create a histogram that reflected grain-size distribution. In both cases, multiple surface locations were interrogated for each sample using a variety of scan sizes ranging from 500 x 500 nm to 10 x 10 μm.

Etch-pit observation was carried out by SEM after selectively removing the Cu and Ta layers by wet chemical treatment. For this purpose, a solution consisting of a 1:1 ratio of nitric acid (HNO_3) and distilled water (H_2O) was employed for Cu removal, while a solution of 20% hydrofluoric acid (HF) in distilled H_2O was employed for removal of the Ta layer. The Si substrates were then exposed for 5 s to a Secco etch solution which consisted of 1 part by volume of 0.15 M potassium dichromate ($K_2Cr_2O_7$) in H_2O and 2 parts HF.[9]

III. RESULTS AND DISCUSSION

A. Characterization of pre- and postannealed Ta films prior to Cu processing

The properties of as-deposited PPCVD Ta, annealed PPCVD Ta, and as-deposited PVD Ta films are summarized in Table II. Prior to Cu deposition and annealing experiments, all types of Ta films were exposed to the same annealing recipe used for the Cu/Ta/Si contact systems, namely, 450 to 650 °C at 50 °C intervals. The purpose of this thermal treatment was to establish baseline

 © 2000 Materials Research Society

TABLE II. Relevant properties for PPCVD and PVD Ta films.

Property (analytical technique)	As-deposited (untreated) PPCVD Ta	Annealed PPCVD Ta (450 °C)	PVD Ta
Thickness (RBS, SEM)	550 Å	550 Å	550 Å
Light element impurities (AES and XPS)	O below detection limits, C < 2.0 at.%	O below detection limits, C < 2.0 at.%	O and C below detection limits
Hydrogen incorporation (hydrogen profiling)	~20 at.%	~0 at.%	~1 at.%
Heavy element impurities (XPS, RBS)	≤2.7 at.% Br, Ar below detection limits	≤2.7 at.% Br, Ar below detection limits	~1 at.% Ar Br below detection limits
Phase identification and texture (XRD)	Polycrystalline β-phase	Polycrystalline β-phase	Polycrystalline β-phase with (001) preferred orientation
Resistivity (four-point probe)	~180 μΩ cm	~180 μΩ cm	~140 μΩ cm
Root-mean-square surface roughness (AFM)	~1.1 nm	~1.1 nm	~0.6 nm
Surface grain size (AFM)	~8.0 nm	~8.0 nm	~11.0 nm

performance metrics and to determine the effects of annealing on key film characteristics, including Br concentration, hydrogen incorporation, film microstructure, and surface morphology.

1. Effects of thermal treatment on Br in PPCVD Ta films

As expected, no Br was observed in the PVD Ta films. In contrast, approximately 2.7 at.% Br was measured by RBS in the as-deposited PPCVD Ta films. As a result, Br stability within the PPCVD Ta matrix was investigated as a function of annealing temperature. Figure 1(a) displays the RBS spectrum of as-deposited PPCVD Ta, while Figure 1(b) shows the same film after exposure to the highest annealing temperature of 650 °C. No change was observed in Br concentration and peak profile after all annealing steps. This finding supports the expectation that Br requires high thermal energy for out-diffusion from Ta and, consequently, is not expected to negatively impact the reliability and stability of the Cu/Ta/Si contact system.

The observed stability of residual Br in Ta is in good agreement with the work of Seel *et al.* [10] They found that the barrier to chlorine (Cl) diffusion in Si was significantly higher than its fluorine (F) counterpart, a behavior attributed to the higher ionicity (larger size) and greater Coulomb interaction for Cl in comparison with F. Similar trends were also seen for the thermally activated diffusion characteristics of iodine (I) and Cl in titanium nitride, with the heavier halide (I) requiring significantly higher activation energy to diffuse than its lighter analog (Cl). [11]

In addition, no variations in the Ta and Si RBS peak heights and profiles were detected, even after annealing at 650 °C. This finding is expected given the known stability of the Ta-Si contact system. [4]

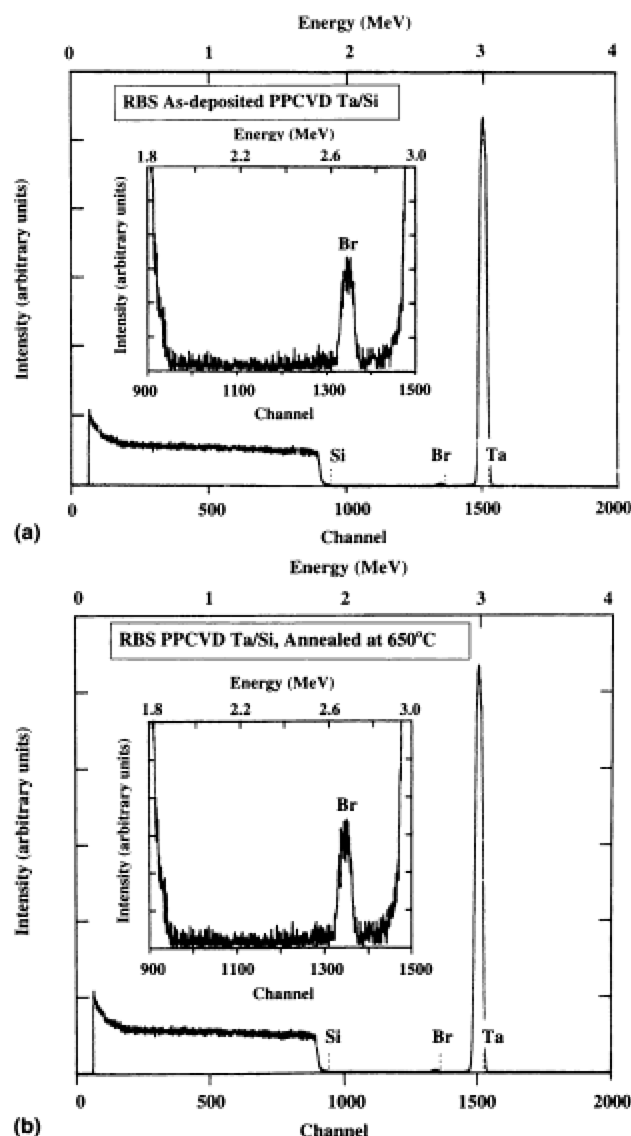

FIG. 1. Typical RBS spectra of PPCVD Ta films: (a) as-deposited and (b) annealed at 650 °C. The Br RBS peak is shown magnified in the insets.

 © 2000 Materials Research Society

2. Effects of thermal treatment on H in PPCVD Ta films

Nuclear reaction analysis (NRA) for hydrogen profiling indicated the absence of hydrogen in PVD Ta. In contrast, NRA yielded approximately 20 at.% H in as-deposited PPCVD Ta, as shown in Fig. 2(a). The incorporation of H in Ta is expected to be in the form of a solid solution, given the solubility limits (up to 30 at.%) of H in Ta. However, the level of hydrogen decreased to below the detection limits of NRA after annealing at 450 °C, as shown in Fig. 2(b), indicating the complete out-diffusion of H from the Ta films.

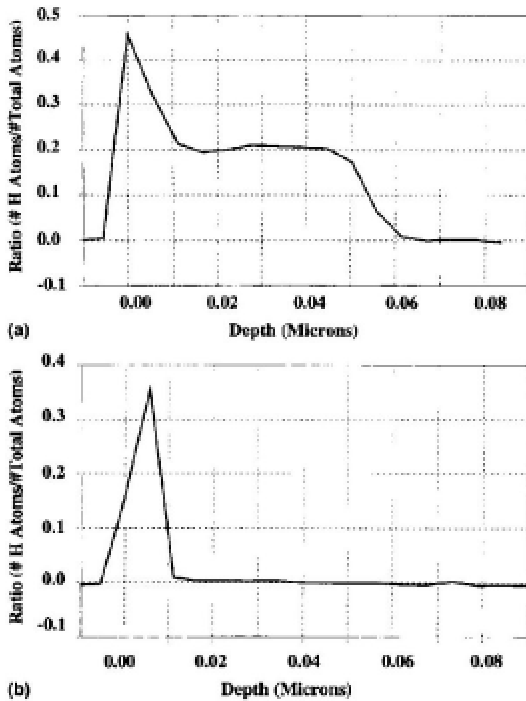

FIG. 2. Hydrogen depth profiles in PPCVD Ta films: (a) as-deposited and (b) annealed at 450 °C.

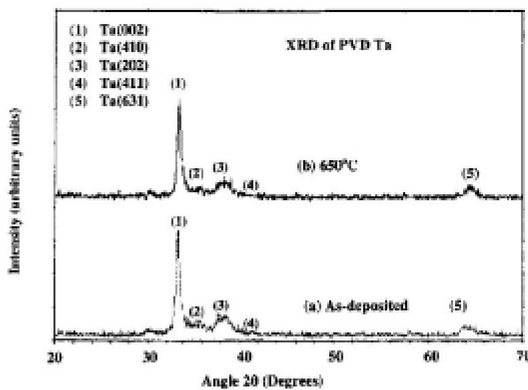

FIG. 3. X-ray diffraction patterns of PVD Ta films: (a) as-deposited and (b) annealed at 650 °C.

3. Effects of thermal treatment on Ta microstructure

Typical XRD spectra for as-deposited and post-annealed (650 °C) PVD Ta films are shown in Figs. 3(a) and 3(b), respectively. The XRD spectrum of as-deposited PVD Ta indicated a polycrystalline tetragonal β Ta phase with a <001> fiber texture. No significant change was observed between the XRD spectra of as-deposited and postannealed PVD Ta films.

Figure 4 displays the XRD spectra for PPCVD Ta films that were treated as follows: (a) no thermal treatment, (b) annealed at 600 °C, and (c) annealed at 650 °C. The XRD profiles of all PPCVD Ta films were practically identical, with all samples exhibiting the characteristic XRD spectrum of a polycrystalline tetragonal β-Ta phase with no preferential orientation. However, the XRD reflection peaks became sharper and exhibited higher intensity after annealing at 650 °C, a behavior that indicates the occurrence of grain growth.

4. Effects of thermal treatment on Ta surface morphology

The AFM measured surface grain size of PPCVD Ta films as a function of annealing

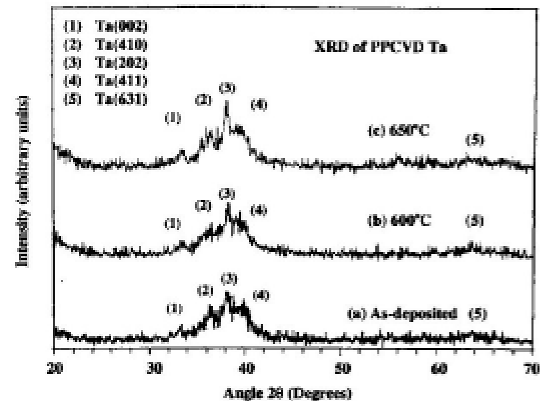

FIG. 4. X-ray diffraction patterns of PPCVD Ta films: (a) as-deposited, (b) annealed at 600 °C, and (c) annealed at 650 °C.

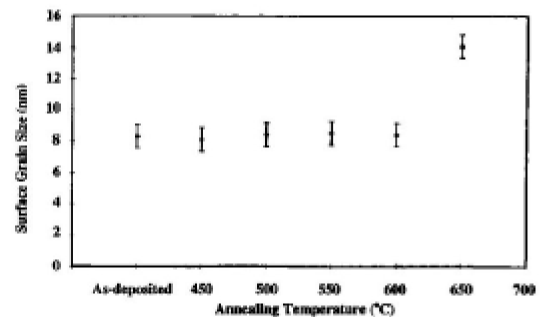

FIG. 5. AFM average surface grain size of PPCVD Ta films as a function of annealing temperature.

 © 2000 Materials Research Society

temperature is plotted in Fig. 5. No marked changes in surface grain size were observed up to 600 °C. However, an increase in the annealing temperature from 600 to 650 °C resulted in a significant enhancement in the AFM measured average surface grain size, from approximately 8 to about 14 nm.

Similarly, Fig. 6 plots the AFM derived rms surface roughness of PPCVD Ta films as a function of annealing temperature. The data indicates an increase of 60% in rms surface roughness, from approximately 1.1 to about 1.8 nm, after the 450 °C annealing step. Further annealing at higher temperature did not generate any additional increase in surface roughness of the PPCVD Ta films, except after the 650 °C annealing step. The latter yielded an increase in surface roughness to 2.7 nm. This trend is consistent with our XRD findings, and it is attributed to the occurrence of grain growth after annealing at 650 °C. In the case of PVD Ta, surface grain size and surface roughness were independent of the annealing temperature.

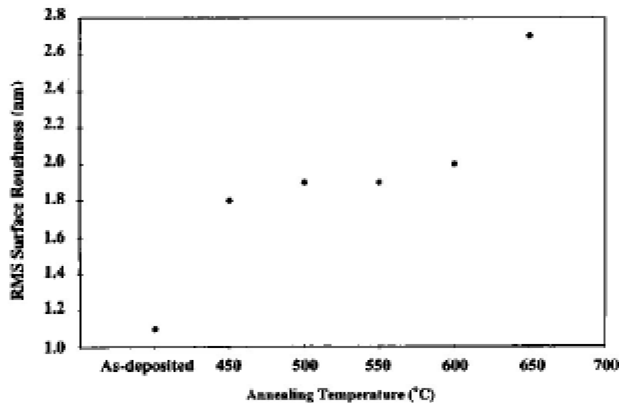

FIG. 6. AFM rms surface roughness of PPCVD Ta films as a function of annealing temperature.

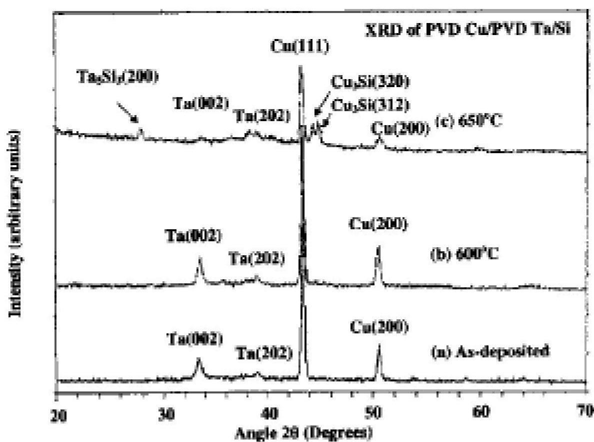
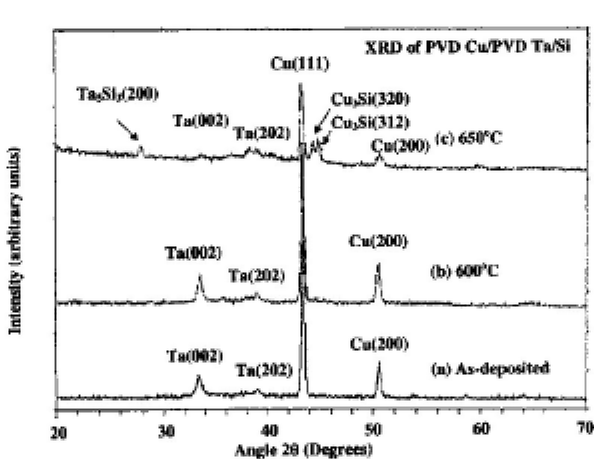

FIG. 7. X-ray diffraction patterns of Cu/PVD Ta/Si stacks: (a) as-deposited, (b) annealed at 600 °C, and (c) annealed at 650 °C.

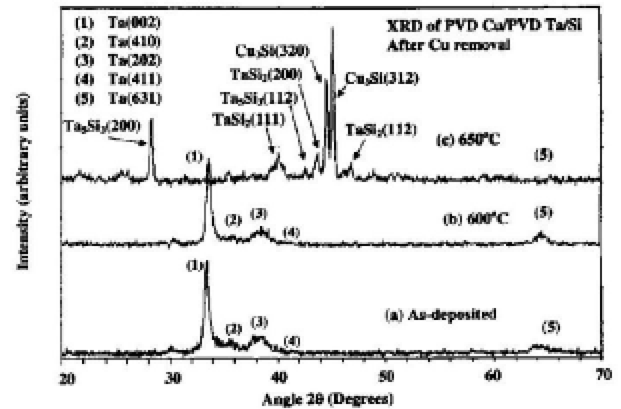

FIG. 8. X-ray diffraction patterns of Cu/PVD Ta/Si stacks: (a) as-deposited, (b) annealed at 600 °C, and (c) annealed at 650 °C. All spectra were collected after Cu removal.

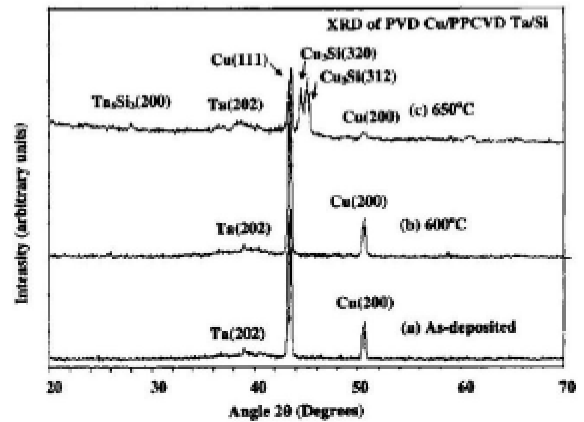

FIG. 9. X-ray diffraction patterns of Cu/PPCVD Ta/Si stacks: (a) as-deposited, (b) annealed at 600 °C, and (c) annealed at 600 °C.

FIG. 10. X-ray diffraction patterns of Cu/PPCVD Ta/Si stacks: (a) as-deposited, (b) annealed at 600 °C, and (c) annealed at 650 °C. All spectra were collected after Cu removal.

 © 2000 Materials Research Society

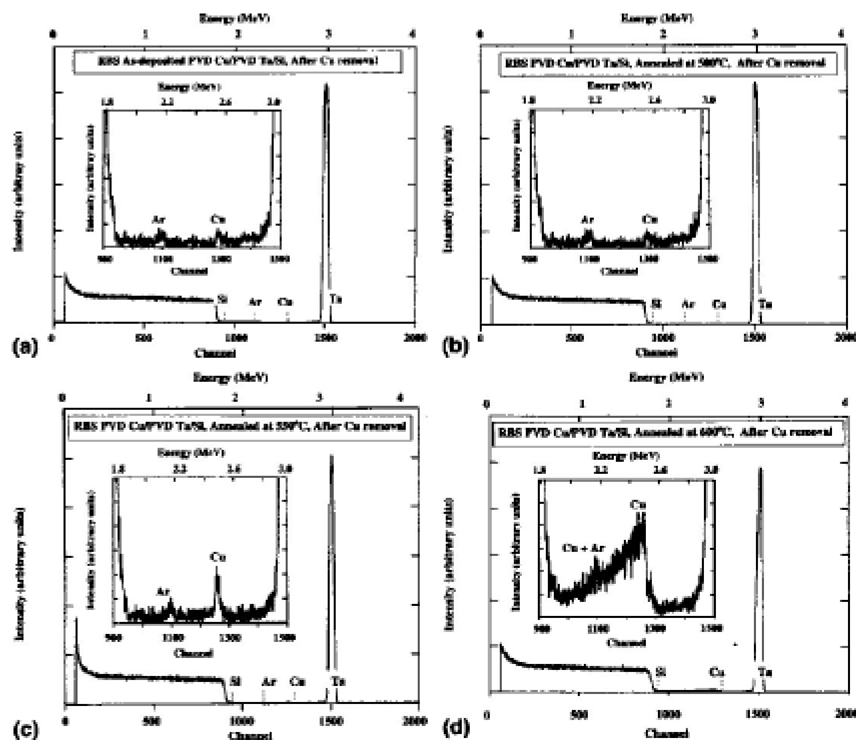

FIG. 11. RBS spectra of Cu/PVD Ta/Si stacks: (a) as-deposited, (b) annealed at 500 °C, (c) annealed at 550 °C, and (d) annealed at 600 °C. All spectra were compiled after Cu removal. The Ar and Cu peaks are shown magnified in the inset.

B. Characterization of diffusion barrier performance of PVD and PPCVD Ta

1. Effects of thermal treatment on the microstructure of Cu/Ta/Si stacks

The microstructure and potential material interactions in Cu/as-deposited PVD Ta/Si, Cu/untreated PPCVD Ta/ Si, and Cu/preannealed PPCVD Ta/Si were examined by XRD. Representative XRD spectra are displayed in Fig. 7 for Cu/PVD Ta/Si stacks which were treated as follows: (a) no thermal treatment, (b) annealed at 600 °C, and (c) annealed at 650 °C. In all cases, strong Cu(111), Cu(200), and β-Ta(002) reflection lines were detected, along with weak and broad peaks corresponding to the β-Ta phase. In addition, XRD detected the presence of Cu_3Si and Ta_5Si_3 after the 650 °C annealing step. This result indicates barrier failure, as evidenced by Cu diffusion to the Si interface and the formation of Cu-Si and Ta-Si compounds.

The XRD studies described above were repeated for each thermal treatment step after removal of the top Cu layer. The purpose was to eliminate any possible XRD peak interference effects that could result from the presence of the thicker Cu overlayer and ensure higher accuracy in the detection of possible thermally induced material interactions. The resulting XRD spectra, as shown in Fig. 8, confirmed the stability of the PVD Ta barrier up to 600 °C. Above that temperature, XRD revealed the existence of a $TaSi_2$ phase, in addition to the Cu_3Si and Ta_5Si_3 phases that were observed prior to Cu stripping.

Representative XRD spectra are displayed in Fig. 9 for Cu/untreated PPCVD Ta/Si stacks which were treated as follows: (a) no thermal treatment, (b) annealed at 600 °C, and (c) annealed at 650 °C. Similarly, Figures 10(a)–10(c) exhibit the XRD profiles of the same samples after Cu stripping. The XRD data indicated that the stacks were structurally stable up to 600 °C, as documented by the absence of any Cu-Si and Ta-Si compounds. However, formation of the Cu_3Si, Ta_5Si_3, and $TaSi_2$ phases was observed after the 650 °C, indicating barrier failure. Similar results were obtained for Cu/pretreated PPCVD Ta/Si stacks, where the PPCVD Ta films were thermally treated at 450 °C in 1-atm of argon for 30 min to ensure complete hydrogen removal prior to Cu deposition and stack annealing.

 © 2000 Materials Research Society

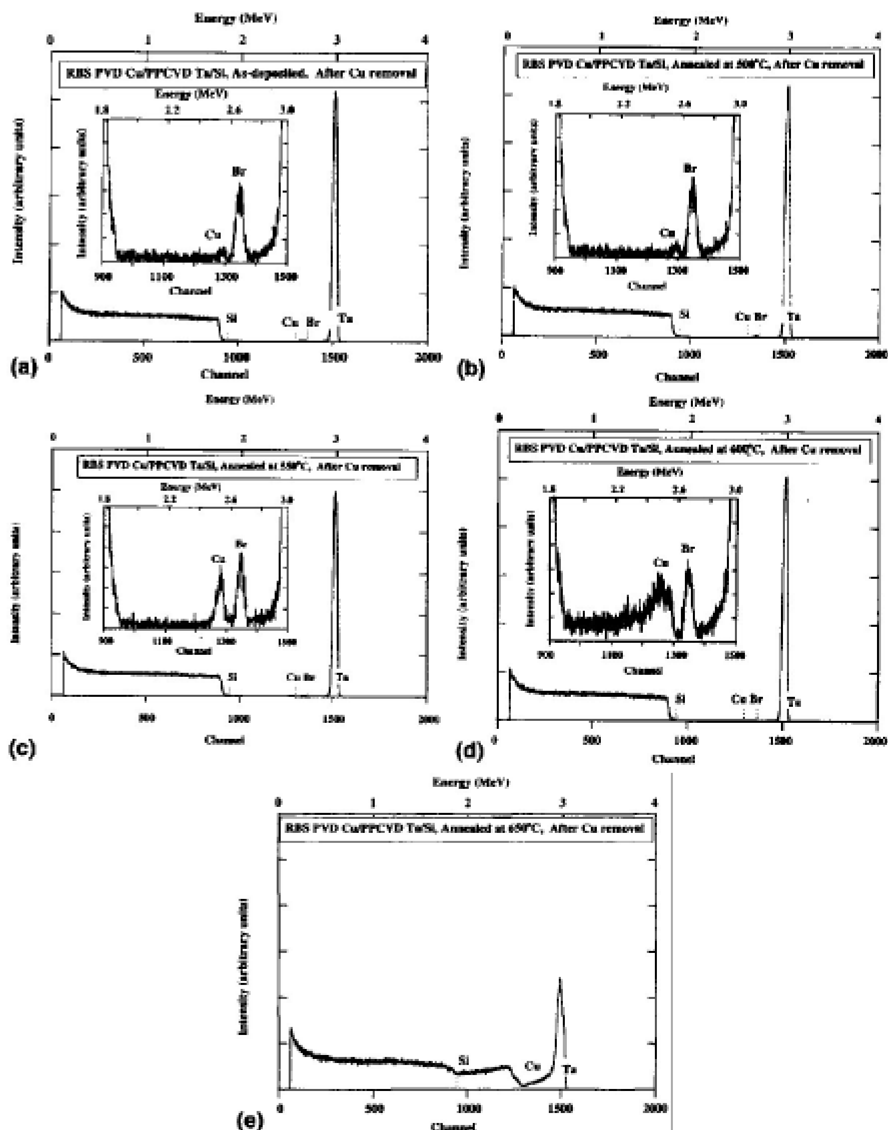

FIG. 12. RBS spectra of Cu/PPCVD Ta/Si stacks: (a) as-deposited, (b) annealed at 500 °C, (c) annealed at 550 °C, (d) annealed at 600 °C, and (e) annealed at 650 °C. All spectra were compiled after Cu removal. The Br and Cu peaks are shown magnified in the inset.

2. Effects of thermal treatment on composition of Cu/Ta/Si stacks

In this part of the study, Cu was stripped from the pre-and postannealed Cu/PVD Ta/Si, Cu/untreated PPCVD Ta/Si, and Cu/preannealed PPCVD Ta/Si stacks prior to RBS analysis. The purpose was to ensure accuracy in RBS compositional results. Representative RBS spectra are displayed in Fig. 11 for Cu/PVD Ta/Si stacks which were treated as follows: (a) no thermal treatment, (b) annealed at 500 °C, (c) annealed at 550 °C, and (d) annealed at 600 °C. As mentioned earlier, the RBS spectra are shown after Cu removal, with magnification of the Ar and Cu peaks being provided in the inset.

No changes were observed in the RBS spectra for stacks annealed up to 500 °C. However, the Cu peak increased in width and intensity with higher annealing temperatures, indicating the gradual diffusion of Cu into Ta. Significant diffusion of Cu into Si was clearly observed after the 600 °C annealing step.

Representative RBS spectra are displayed in Fig. 12 for Cu/untreated PPCVD Ta/Si stacks which were treated as follows: (a) no thermal treatment, (b) annealed at 500 °C, (c) annealed at 550 °C, and (d) annealed at 600 °C. The RBS spectra were compiled after Cu stripping, with magnification of the Cu and Br peaks being provided in the inset. As in the case of PVD Ta, no changes were observed in the RBS spectra for stacks annealed up to 500 °C. However,

 © 2000 Materials Research Society

the Cu peak increased in width and intensity with higher annealing temperatures, indicating the gradual diffusion of Cu into Ta. Significant diffusion of Cu into Si was clearly observed after the 600 °C annealing step. Similar results were obtained for Cu/pretreated PPCVD Ta/Si stacks, where the PPCVD Ta films were thermally treated at 450 °C in Katz argon for 30 min to ensure complete hydrogen removal prior to Cu deposition and stack annealing.

3. Secco etch pit observation

RBS studies indicated that the Cu/PVD Ta/Si, Cu/untreated PPCVD Ta/Si, and Cu/pretreated PPCVD Ta/ Cu stacks were structurally stable, with no Cu being detected in the underlying Si substrate, up to 550 °C. However, due to sensitivity limitations in RBS analysis, Secco etch treatment and subsequent inspection by SEM were implemented to document the onset temperature of diffusion of Cu into Si. Etch-pit observation using the Secco etch has been shown to be more sensitive to the detection of the initial stages of Cu diffusion into Si than the analytical techniques listed above.13

Typical SEM micrographs of the Si surface are shown in Fig. 13 after Secco etch of Cu/PVD Ta/Si stacks that were annealed as follows: (a) 550 °C and (b) 600 °C. The samples annealed at 550 °C exhibited a smooth and clean Si surface. However rectangular-shaped etch pits, with sizes on the order of a few microns, were detected after the 600 °C annealing step. The precipitates around the etch pits are believed to be Cu silicides.[13]

Secco etching of the Cu/pretreated PPCVD Ta/Si contact systems yielded a similar result, with etch pits being observed only after the 600 °C annealing step. In contrast, the Cu/untreated PPCVD Ta/Si contact system failed above 500 °C, as documented by the observation of etch pits in Si after the 550 °C annealing step. This result is illustrated in the SEM micrographs of Fig. 14, which displays the morphology of the Si surface after Secco etch of Cu/untreated PPCVD Ta/Si stacks that were annealed as follows: (a) 500 °C, (b) 550 °C, and (c) 600 °C.

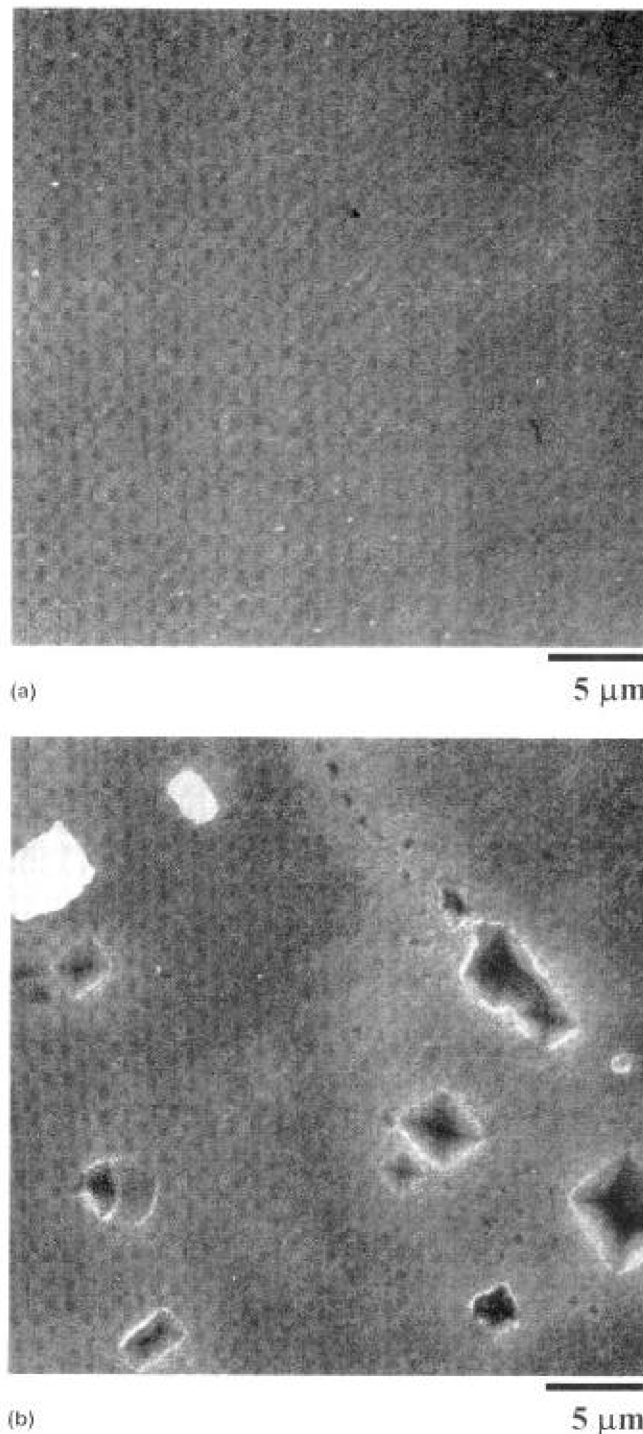

FIG. 13. SEM micrographs of the Si surface after Secco etch for Cu/PVD Ta/Si stacks annealed at the following temperatures: (a) 550 °C and (b) 600 °C.

C. Discussion

The results reported above indicate that PVD Ta and thermally pretreated PPCVD Ta films act as a good diffusion barrier between Cu and Si up to 550 °C. The PPCVD Ta Ellms were thermally treated at 450 °C in l-atm argon for 30 min to ensure complete hydrogen removal prior to Cu deposition and stack annealing. In contrast, untreated PPCVD Ta films exhibited thermal stability up to 500 °C only.

In terms of breakdown mechanisms, our findings for both PVD and PPCVD Ta are consistent with the

 © 2000 Materials Research Society

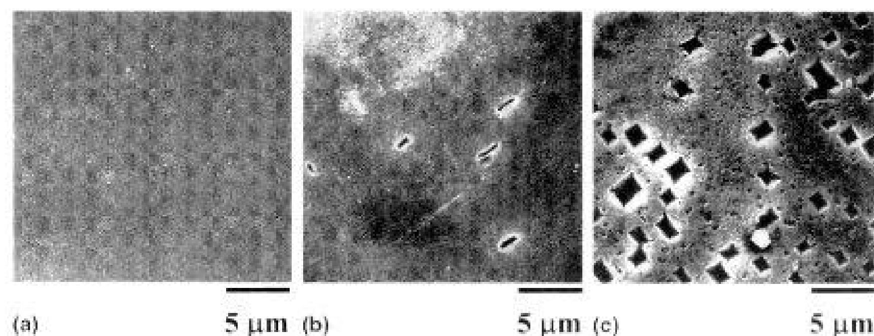

FIG. 14. SEM micrographs of the Si surface after Secco etch for Cu/PPCVD Ta/Si stacks annealed at the following temperatures: (a) 500 °C, (b) 550 °C, and (c) 600 °C.

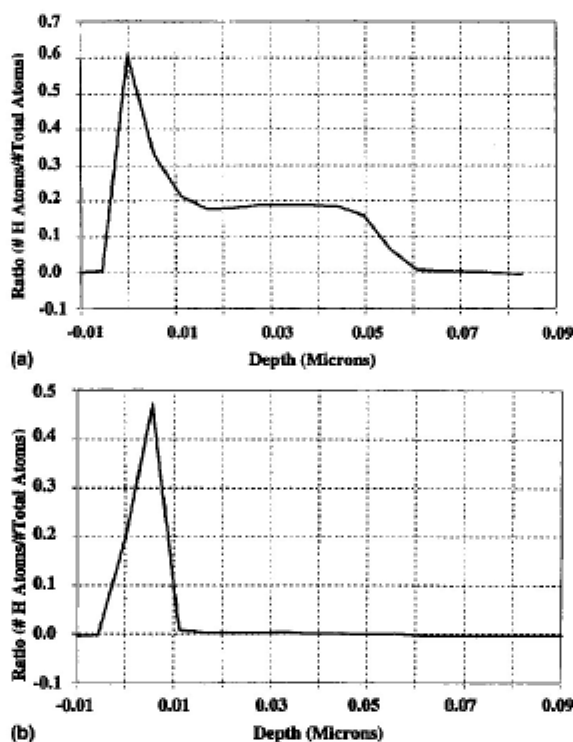

FIG. 15. Hydrogen depth profiles for Cu/PPCVD Ta/Si stacks: (a) as-deposited and (b) annealed at 450 °C. Spectra were compiled after Cu removal.

failure mechanisms previously reported by Min *et al.*[14] and Holloway *et al.*[15] In particular, the studies by Min *et al.* indicated that failure of the Ta barrier occurs through the migration of Cu into Si rather than an interfacial reaction between Ta and Si. Similarly, Holloway *et al.* reported Ta out-diffusion to the Cu surface after annealing of Cu/PVD Ta/Si stacks at 550 °C, a step which was followed by Cu migration through the Ta layer and its subsequent reaction with Si to form Cu_3Si.

These observations are supported by our RBS and Secco etch results, which showed that Ta films without a Cu overlayer did not react with the Si substrate, even after annealing at 650 °C. They are also in agreement with our XRD findings, which did not detect any Ta-Si phases for uncapped PVD Ta/Si and PPCVD Ta/Si stacks, even after annealing at 650 °C. By contrast, PVD Ta and PPCVD Ta barrier failure occurred at lower temperatures in the presence of a CU capping layer, which was accompanied by the formation of Cu-Si and Ta-Si compounds. It is suggested that the diffusing Cu species may be instrumental in the breakage of Si-Si bonds, leading to the formation of vacancies and other defects in the Si lattice. These defects in turn facilitate the silicidation of Ta films.[15]

The reduced barrier effectiveness for untreated PPCVD Ta films cannot be attributed to the presence of bromine. This observation is supported by the fact that pretreated PPCVD Ta and PVD Ta films exhibited similar barrier performance, in spite of the presence of equivalent amounts of Br in the untreated and pretreated PPCVD Ta films. In addition, no variations in Br concentration or peak profile were observed even after thermal treatment at 650 °C. The high thermal stability of Br was independent of the presence of the Cu capping layer, as supported by our RBS data. The same conclusion applies to other potential impurities in the PPCVD Ta films, given that their concentrations were too small to significantly influence barrier properties.

The observed variations in the thermally induced diffusion barrier behavior of the PVD and PPCVD Ta films cannot be attributed to microstructural differences between the two types of Ta films either. No changes were detected in the texture or morphology of the PVD and PPCVD Ta films as a function of annealing temperature. Instead, both Ta films were stable under the thermal treatment conditions investigated.

Bai et *al.*[16] have reported that barrier effectiveness could be affected by surface roughness

 © 2000 Materials Research Society

of the barrier, if the value of roughness is on the order of the film thickness. This was attributed to the presence of short diffusion paths for Cu migration through the barrier. However, surface roughness in the PPCVD Ta films did not exceed 2.7 nm and was thus less than 5% of actual film thickness. This observation eliminates surface roughness as a potential factor in the observed difference in barrier performance.

Alternatively, it is suggested that the out-diffusion of hydrogen from the PPCVD Ta films during thermal annealing might have caused their inferior barrier performance. This suggestion is supported by complete hydrogen removal after annealing at 450 °C, a behavior that was detected in the as-deposited Ta films prior to Cu deposition (Fig. 2). It is also supported by the fact that PPCVD Ta films that were pretreated at 450 °C in argon to ensure the complete removal of hydrogen (see Fig. 15) exhibited a diffusion barrier performance that was equivalent to their PVD Ta counterparts. However, all analytical studies were inconclusive in terms of elucidating the specific structural or chemical changes that resulted from the thermally activated hydrogen out-diffusion and which led to the accelerated barrier failure for as-deposited PPCVD Ta.

It is thus clear that one possible solution for improving the barrier effectiveness of PPCVD Ta films is to implement a 450 °C annealing step prior to Cu deposition, to drive out hydrogen from the Ta matrix. The Cu/untreated PPCVD Ta/Si contact system was thermally stable up to 500 °C, a temperature in excess of those encountered during the device fabrication flow, especially in interconnect schemes which incorporate thermally labile, low dielectric constant materials. This temperature requirement, when combined with the superior step coverage provided by PPCVD Ta in comparison with its PVD counterparts ensures that as-deposited, untreated PPCVD Ta is a viable approach for incorporation in emerging Cu/low dielectric constant metallization schemes.

IV. CONCLUSIONS

A systematic evaluation was carried out of the barrier performance of Ta films grown by PVD and PPCVD using pentabromotantalum and hydrogen as coreactants. The study indicated that the PVD Ta films, and PPCVD Ta films that were hydrogen-free after a preannealing step at 450 °C, were stable against Cu diffusion into Si up to 550 °C. In contrast, untreated PPCVD Ta films exhibited barrier failure above 500 °C. The poorer performance of the untreated PPCVD Ta films could not be attributed to the presence of bromine, given the high thermal stability of Br against migration, even at temperatures in excess of 650 °C. Instead, it is suggested that the out-diffusion of hydrogen from the PPCVD Ta films might have caused their inferior barrier performance. However, all analytical studies were inconclusive in terms of elucidating the specific structural or chemical changes that resulted from the thermally activated hydrogen out-diffusion and which led to the accelerated barrier failure for as-deposited PPCVD Ta.

ACKNOWLEDGMENTS

The work was partially supported by the Semiconduc tor Research Corporation (SRC) Center for Advanced Interconnect Science and Technology (CAIST) and the New York State Center for Advanced Thin Film Tech nology (CAT). This support is gratefully acknowledged.

REFERENCES

1. *The National Technology Roadmap for Semiconductors* (Semiconductor Industry Association, San Jose, CA, 1997).
2. M. Takeyama, A. Noya, T. Sasse, and A. Ohta, J. Vac. Sci. Technol. B **14**, 674 (1996).
3. *CRC Handbook of Chemistry and Physics,* 71st ed., edited by D. Lide (CRC Press, Boston, MA, 1990–1991), pp. 4–109.
4. J.S. Reid, E. Kolawa, and M. Nicolet, J. Mater. Res. **7**, 2424 (1992).
5. M.T. Wang, Y.C. Lin, and M.C. Chen, J. Electrochem. Soc. **145**, 2538 (1998).
6. R.A. Roy, P. Catania, K.L. Saenger, J.J. Cuomo, and R.L. Lossy, J. Vac. Sci. Technol. B **11**, 1921 (1993).
7. X. Chen, H.L. Frisch, and A.E. Kaloyeros, J. Vac. Sci. Technol. B **16**, 2887 (1998).
8. X. Chen, Ph.D. Thesis, University at Albany-SUNY (1998).
9. F. Secco d'Aragona, J. Electrochem. Soc. **119**, 948 (1972).

 © 2000 Materials Research Society

10. M. Seel and P.S. Bagus, Phys. Rev. B **28**, 2023 (1983).
11. C. Faltermeier, C. Goldberg, M. Jones, A. Upham, D. Manger, G. Peterson, J. Lau, and A.E. Kaloyeros, J. Electrochem. Soc. **144**, 2023 (1997).
12. P.N. Baker, Thin Solid Films **14**, 3 (1972).
13. K.C. Park, K.B. Kim, I.J.M.M. Raaljmakers, and K. Ngan, J. Appl. Phys. **80**, 5874 (1996).
14. K.H. Min. K.C. Chun, and K.B. Kim, J. Vac. Sci. Technol. B **14**, 145 (1992).
15. K. Holloway, P.M. Freyer, and C. Cabral, Jr., J. Appl. Phys. **71**, 5433 (1992).
16. G. Bai, S. Wittenbrock, V. Ochoa, C. Chiang, and M. Bohr, in *Polycrystalline Thin Films: Structure, Texture, Properties and Applications II,* edited by H.J. Frost, M.A. Parker, C.A. Ross, and E.A. Holm (Mater. Res. Soc. Symp. Proc. **403**, Pittsburgh, PA, 1996), p. 501.

 © 2000 Materials Research Society